Contents lists available at ScienceDirect

Composites: Part A

journal homepage: www.elsevier.com/locate/compositesa

Experimental determination of the permeability of engineering textiles: Benchmark II

N. Vernet [a], E. Ruiz [a,*], S. Advani [b], J.B. Alms [b], M. Aubert [c], M. Barburski [d], B. Barari [e], J.M. Beraud [c], D.C. Berg [f], N. Correia [g], M. Danzi [h], T. Delavière [i], M. Dickert [f], C. Di Fratta [h], A. Endruweit [j], P. Ermanni [h], G. Francucci [k], J.A. Garcia [l], A. George [m], C. Hahn [n], F. Klunker [h], S.V. Lomov [d], A. Long [j], B. Louis [h], J. Maldonado [h], R. Meier [n], V. Michaud [i], H. Perrin [o], K. Pillai [e], E. Rodriguez [k], F. Trochu [a], S. Verheyden [i], M. Wietgrefe [p], W. Xiong [h], S. Zaremba [n], G. Ziegmann [f]

[a] Chair on Composites of High Performance, École polytechnique de Montréal, Canada
[b] Department of Mechanical Engineering, University of Delaware, USA
[c] Hexcel Reinforcements, Les Avenieres, France
[d] Department of Metallurgy and Materials Engineering, KU Leuven, Belgium
[e] Mechanical Engineering Department, University of Wisconsin, USA
[f] Institut für Polymerwerkstoffe und Kunststofftechnik, Technische Universität Clausthal, Germany
[g] Campus da FEUP, Universidade do Porto, Portugal
[h] Centre of Structure Technologies, Eidgenössische Technische Hochschule Zürich, Switzerland
[i] Laboratoire de technologie des Composites et Polymères, École Polytechnique Fédérale de Lausanne, Switzerland
[j] Division of Materials, Mechanics and Structures, University of Nottingham, UK
[k] Institute of Material Science and Technology, National University of Mar del Plata, Argentina
[l] Universitat Politecnica de Valencia, Spain
[m] Swerea SICOMP, Öjebyn, Sweden
[n] Institute for Carbon Composites, Faculty of Mechanical Engineering, Technische Universitaet Muenchen, Garching, Germany
[o] Pôle de Plasturgie de l'Est, PPE, France
[p] Airbus Operations GmbH, Bremen, Germany

ARTICLE INFO

ABSTRACT

In this second international permeability benchmark, the in-plane permeability values of a carbon fabric were studied by twelve research groups worldwide. One participant also investigated the deformation of the tested carbon fabric. The aim of this work was to obtain comparable results in order to make a step toward standardization of permeability measurements. Unidirectional injections were thus conducted to determine the unsaturated in-plane permeability tensor of the fabric. Procedures used by participants were specified in the guidelines defined for this benchmark. Participants were asked to use the same values for parameters such as fiber volume fraction, injection pressure and fluid viscosity to minimize sources of scatter. The comparison of the results from each participant was encouraging. The scatter between data obtained while respecting the guidelines was below 25%. However, a higher dispersion was observed when some parameters differed from the recommendations of this exercise.

© 2014 Elsevier Ltd. All rights reserved.

1. Introduction

Liquid Composite Molding (LCM) processes are increasingly used in the automotive and aeronautic industries. Five common steps in LCM are necessary to manufacture a composite part. Firstly, the fibrous reinforcement is preformed to the desired geometrical shape. Then, it is placed in the mold cavity. A flexible or rigid top is used to close the mold in order to inject the polymeric resin in the next step. Once the mold is completely filled, the injection is discontinued allowing the resin to cure after which the composite is demolded.

The filling of complex-shaped molds is a critical step. Indeed, dry zones (region not covered by resin) may appear if specifications like positions of injection and vent gates, injection pressure and clamping force are not well defined. Mold filling simulation

softwares such as PAM-RTM [1], LIMS [2] and Polyworx [3] allow one to predict the resin flow and filling time, the flow front shapes, the pressure and velocity fields of the complete manufacturing process. A complete characterization of the material properties is necessary to run such simulations.

The permeability of fibrous reinforcement is one of the key parameters governing the mold filling. It corresponds to the ease of a fluid to flow through a porous medium. This property was first identified by Darcy [4] in 1856 in the form of hydraulic conductivity. Based on the observation of water flowing through a vertical column of sand, an empirical formula now known as Darcy's law was derived:

$$v = -\left(\frac{K}{\mu}\right) \cdot \nabla P \tag{1}$$

where v, μ, ∇P and K are respectively the volume averaged Darcy velocity, the dynamic fluid viscosity, the pressure gradient across the porous medium and the permeability. In porous media such as fibrous reinforcements, the permeability is anisotropic. Thus the second order tensor describing this property can be written as:

$$K = \begin{bmatrix} K_{xx} & K_{xy} & K_{xz} \\ K_{yx} & K_{yy} & K_{yz} \\ K_{zx} & K_{zy} & K_{zz} \end{bmatrix} \tag{2}$$

This tensor can be diagonalized to obtain the three principal permeability values of a fibrous reinforcement. It is typically assumed that the first two principal permeability K_1 and K_2 lie in the plane of the fiber bed while the third one K_3 is oriented through it thickness. The in-plane flowing pattern is thus an ellipse oriented at an angle β which can be defined as the angle between the warp direction and the principal flow direction as shown in Fig. 1 (extracted from [5]). In-plane principal permeability values are of particular interest because in several composite manufacturing processes are performed injecting resin in the plane of the fibrous reinforcement.

A wide variety of methods and approaches have been developed to determine the in-plane permeability of a fibrous reinforcement. Firstly, it is possible to apply models to estimate the permeability. Kozeny and Carman [6] and Gebart [7] have developed equations taking into account geometrical parameters and the solid volume fraction to calculate the permeability of a single scale porous medium. This kind of model is still used to approximate the permeability of a fiber tow. However, they are not well adapted to determine the permeability of dual scale porous media such as fabric. Thus, more complex analytical models, such as for example Lundström [8] or Papathanasiou [9], have been created considering the fibrous

reinforcement as a medium composed of fiber tows. Thus, the flow was divided in two components: the mainly capillary flow in the tows and the viscous flow between the tows. Numerical simulations have also been developed to calculate the permeability of a fibrous reinforcement. Various techniques have been explored: lattice Boltzmann method [10], finite differences calculation [11,12] and the finite element method [13–16]. However, to validate all these models, experimental permeability data are necessary.

As summarized in [17], numerous experimental techniques have been developed and described in the scientific literature. Two of them are commonly used to determine K_1 and K_2: unidirectional [5,18] and radial techniques [19,20]. Both methods show advantages and drawbacks. The former method has a higher repeatability thanks to an easier tracking of the straight unidirectional flow front. Moreover, the experiment is less complicated to set up since the flow front is straight. This method can be used to determine both unsaturated permeability by following the flow front and saturated permeability after the flow has filled the entire preform. However, the radial method permits the determination of the unsaturated permeability ellipse with only one experiment. In addition, the possible race-tracking observed in a unidirectional measurement [21] is avoided here.

The lack of standardization of permeability measurements impedes researchers from comparing permeability obtained from different experimental setups. Parnas et al. [22] and Lundström et al. [23] have respectively initiated the creation of a permeability database and organized a small-scale benchmark. Their efforts were important, but the involvement of a larger part of the research community is necessary to take a step towards standardization. A first international permeability benchmark exercise [24], initiated by ONERA (Office National d'Étude et de Recherche Aérospatiales, France) and KU Leuven, was conducted for this purpose. The aim was to get an overview of the methods, practical uses and range of results obtained by different participants worldwide. The permeability data of twelve institutions from six countries were compiled and compared for two different fabrics. The main finding of this study was a significant scatter of more than one order of magnitude between all participants for both reinforcements tested. The explanation then was that human factors such as skilled and experienced personnel, preparation of specimens or evaluation of raw data were principally responsible for this scatter. In that work, it was suggested that another benchmark based on a common procedure and more controlled experimental conditions needed to be conducted in order to confirm the causes of the scatter and allow a better comparison of experimental results.

For this purpose, a guideline document [25] was written in a collaborative effort among the participants of this first exercise. In these guidelines, test conditions for unidirectional unsaturated permeability measurements are defined. Based on them and the common desire of researchers to standardize the determination of permeability, it was agreed to conduct a second benchmark with the support of Hexcel Fabrics. A total of twelve participants (see details in Table 1) were invited to carry out the in-plane unsaturated permeability measurements of a carbon fabric using their respective setups and following the guidelines of this benchmark. As the unidirectional method was chosen, three directions of measurement were necessary to obtain the in-plane ellipse of permeability [5]. Thus, nine institutions were able to carry out these measurements and obtain the permeability ellipse. This paper presents the procedure used, the experimental conditions adhered to and the results obtained by each participant. The permeability values were analyzed and compared in order to determine the scatter of values occurring with the stated guidelines. Finally, a short comparison with the first benchmark was performed and concluding remarks are presented regarding permeability measurements.
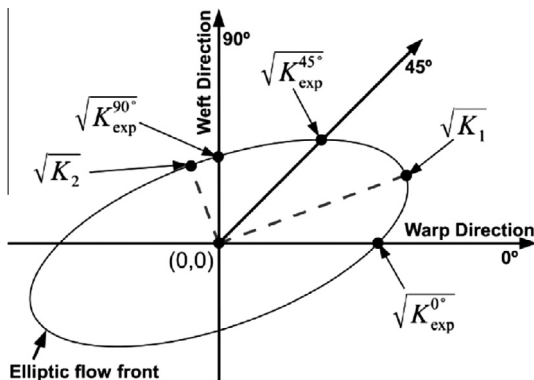

Fig. 1. Elliptic pattern of a fluid flowing through a fibrous reinforcement [5].

Table 1
Participants in the benchmark exercise.

Institution	Division	Country	Referred to as
École Polytechnique de Montréal	Chair on Composites of High Performance	Canada	CCHP
Technische Universität Clausthal	Institut für Polymerwerkstoffe und Kunststofftechnik	Germany	Clausthal
University of Delaware	Department of Mechanical Engineering	USA	Delaware
National University of Mar del Plata	Institute of Material Science and Technology	Argentina	INTEMA
École Polytechnique Fédérale de Lausanne	Laboratoire de technologie des Composites et Polymères	Switzerland	Lausanne
KU Leuven[*]	Departement of Metallurgy and Materials Engineering	Belgium	Leuven
University of Wisconsin	Department of Mechanical Engineering	USA	Milwaukee
Technische Universitaet Muenchen	Institute for Carbon Composites	Germany	Munich
University of Nottingham	Division of Materials, Mechanics and Structures	United Kingdom	Nottingham
Pôle Plasturgie de l'Est	R&D department	France	PPE
SICOMP	Swerea	Sweden	Sicomp
Universitat Politècnica de Valencia	Instituto de Diseño para la Fabricación	Spain	Valencia
Eidgenössische Technische Hochschule Zürich	Centre of Structure Technologies	Switzerland	Zurich

[*] Investigate the deformation of the fabric.

2. Permeability measurement

2.1. Material specifications

2.1.1. Reinforcement

As in the first permeability benchmark, the reinforcement chosen is a 2×2 twill carbon fabric provided by Hexcel Fabrics with an areal density of 285 g/m². It is composed of 6 K fiber tows in both warp and weft directions. The fabric properties are summarized in Table 2. The fabric measurements were performed according to ISO 10120:1991 and ISO 3801:1977. It can be noticed that, as specified by the manufacturer, the number of tows per centimeter in the warp and weft directions is similar regarding the mean values and standard deviations obtained.
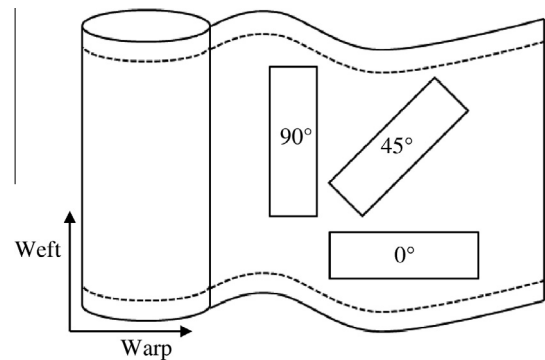
As displayed in Fig. 2, testing directions at 0° and 90° were defined respectively in the warp and weft of the roll. The 45° testing orientation was obtained between the 0° and 90° directions. This upfront definition allows the comparison of the unidirectional effective permeability of all participants.

2.1.2. Testing fluid

Thermosetting resins typically used in composite manufacturing show a Newtonian behavior prior to gelation [26,27]. However,

Table 2
Details on reinforcement architecture.

Manufacturer	Hexcel Fabrics	
Fabric	G0986 D1200 Carbon fabric	
	Data sheet	Measured
Weave	2×2 twill	
Areal density (g/m²)	285	284 ± 2
Fiber density (g/m³)	1.78*10⁶	
Nominal construction	Warp: 3.5	3.52 ± 0.07
(tows/cm)	Weft: 3.5	3.46 ± 0.07
Weight distribution	Warp: 50%	
	Weft: 50%	
Tows warp and weft	Carbon HT	
Type	HTA 5131 6 K	
Filament diameter (µm)	7	
Linear density (tex)	400	419 ± 15
Tow width (mm)	n/a	Warp: 2.31 ± 0.17 Weft: 2.27 ± 0.20
Image		

Fig. 2. Directions for cutting in the reinforcement roll.

viscosity may vary due to solvent evaporation or cure reaction. Thus, the use of a test fluid instead of resin is usually recommended in order to perform experiments in a more reproducible manner. For this reason, a calibrated silicone oil was recommended as the testing fluid for this benchmark. Table 3 summarizes the test fluids used by each participant of the exercise. Only three participants have chosen a different fluid: corn syrup for Delaware, motor oil for Milwaukee and a synthetic oil for Nottingham. Fluid properties were verified by most participants before the experiments. The majority of them have also verified the Newtonian behavior of the testing fluid. The targeted viscosity of the fluid was fixed to 0.1 Pa s. The effective viscosity varies between 0.088 and 0.220 Pa s as given in Table 3.

2.2. Experimental setups

In this study, experimental setups were composed of two rigid mold surfaces as a standard RTM (Resin Transfer Molding) mold. Top molds were transparent (acrylic, glass, etc.) to be able to observe the fluid flowing through the reinforcement while bottom molds were opaque (aluminum or steel). Between these two parts, the thickness was fixed using frames or shims as shown schematically in Fig. 3 (extracted from [28]). A sealing rubber was also placed between the mold surfaces in order to prevent any leak during the measurement. The testing fluid was injected from the injection gate on one side of the sample along the longitudinal direction of the mold. The setup used by each participant is detailed in Table 4.

Sample size is another key parameter that has to be chosen wisely. The size of the fibrous material must be several times larger than the unit cell of the woven fabric. In fact, sample size has to be larger than the Representative Elementary Volume (REV) of the

Table 3
List of testing fluids used by each participant.

Institution	Test fluid	Determination of viscosity	Temperature (°C)	Viscosity (Pa s)	Additional comments
CCHP	Silicone oil	T measured before test μ from $\mu(T)$ curve	23–23.9	0.100–0.101	Newtonian behavior verified
Clausthal	Silicone oil	μ from $\mu(T)$ curve	18.6–23.8	0.096–0.104	Newtonian behavior verified
Delaware	Corn syrup	–	23.1–23.3	0.098–0.160	–
INTEMA	Silicone oil	T measured before test μ from $\mu(T)$ curve	13–19.2	0.106–0.122	–
Lausanne	Silicone oil	T measured before test μ from $\mu(T)$ curve	21.5–22	0.088	Newtonian behavior verified
Milwaukee	Motor oil	T measured before test μ from $\mu(T)$ curve	20.5–23	0.200–0.220	–
Munich	Silicone oil	T measured before test μ from $\mu(T)$ curve	12.4–21	0.124–0.142	Newtonian behavior verified
Nottingham	Synthetic oil	T measured before test μ from $\mu(T)$ curve	20–21.5	0.095–0.103	Newtonian behavior verified
PPE	Silicone oil	–	–	0.100	–
Sicomp	Silicone oil	T measured before test μ from $\mu(T)$ curve	18.5–19.8	0.100–0.101	Newtonian behavior verified
Valencia	Silicone oil	–	25.5	0.100	–
Zurich	Silicone oil	T measured in the mold μ from $\mu(T)$ curve	22.8–25.5	0.101–0.106	Newtonian behavior verified
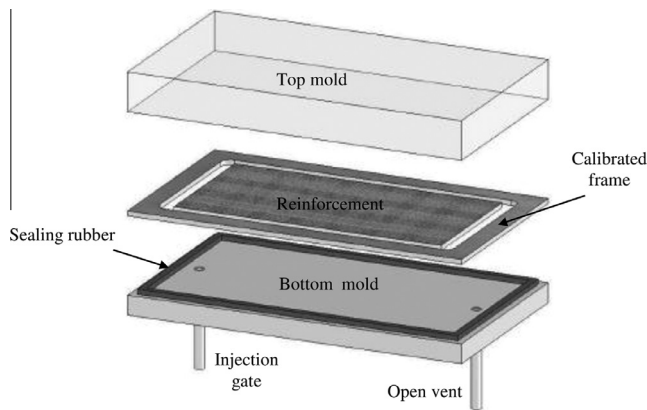
Fig. 3. Typical test mold as described in [28].

fabric to avoid any influence of the stochastic non-uniformity of the weaving pattern. Moreover, the length and the width of the sample plays an important role since the fluid flowing in a short and wide sample (low aspect ratio) easily diverges from the unidirectional condition required [23,29,30]. Also, the flow through a too narrow sample can be highly influenced by the race-tracking. For a good uniformity, a minimal dimension of 400 mm in length and 100 mm in width (aspect ratio of 4) was suggested for this study. A fixed fiber volume fraction (V_f) of 45% was also suggested

for these tests. The number of fabric layers also influences the permeability value. Fiber nesting and non-uniform compaction of the layers cause the intra tow spaces to differ for different numbers of stacked layers. To reduce variability, the number of layers and hence the mold cavity thickness were fixed for this experiment. A total of 10 layers was suggested for each direction as well as a cavity height of 3.5 mm in order to obtain a V_f close to 45%. Some of the participants could not obtain this cavity thickness due to their existing setups. Hence, the number of layers in the preform was adjusted in order to be as close as possible to the desired fiber volume fraction (see Table 4).

When measuring the unsaturated permeability of a dual scale porous media, one must pay special attention to the flow velocity at the flow front. Saturation of the fabric is a combination of the Stokes flow occurring principally within inter-tow spaces and the capillary flow inside the tows. The unsaturated permeability of the fabric is then a consequence of the Stokes versus capillary flow ratio. Varying the injection pressure has a direct impact on the fluid velocity and hence on the unsaturated permeability value of the fabric. To ensure testing the fibers under same flow conditions [31,32], an average capillary number has to be fixed (see Eq. (3)):

$$Ca = \frac{\mu \cdot v_f}{\gamma \cdot \cos\theta} \tag{3}$$

where v_f is the flow velocity, θ the contact angle between the resin and the fibers and γ the surface tension of the resin. Since the test fluid has already been specified as a silicone oil with similar prop-

Table 4
Details on tool setup used by participants.

Institution	Sample size (mm²)	Length/width ratio	Thickness (mm)	Number of layer	Tool material	Reported closing/deflection
CCHP	400*100	4.0	3.60	10	Steel (bottom) Glass (top)	Thickness variation: 1.1%
Clausthal	240*120	2.0	3.50	10	Steel (bottom) Glass (top) + steel stiffeners	Thickness variation: ⩽1%
Delaware	457*142	3.2	3.18	10	Aluminum (bottom) Acrylic (top) + steel stiffening structure	–
INTEMA	400*100	4.0	3.50	10	Steel (bottom) Glass (top)	Thickness variation: 1.4% Mold deflection: 0.1%
Lausanne	250*63	4.0	2.84	8	Steel (bottom) Glass (top) + steel frame	Thickness variation: 1.8% Mold deflection: 0.1%
Milwaukee	1200*178	6.7	10.00	28	Aluminum (bottom) Polycarbonate (top)	Thickness variation: 0.5% Mold deflection: ⩽0.1%
Munich	380*192	2.0	3.50	10	Steel, 35 mm (bottom) Polycarbonate, 40 mm (top)	–
Nottingham	280*114.5	2.5	3.50	10	Steel, 25.3 mm (bottom) Acrylic, 25.6 mm (top)	Thickness variation: 0.9%
PPE	300*100	3	3.50	10	Aluminum (bottom) Polycarbonate (top)	Thickness variation: ⩽2% Mold deflection: ⩽2%
Sicomp	300*150	2.0	3.50	10	Steel, 25 mm (bottom) Acrylic, 80 mm (top)	Thickness variation: 0.4% Mold deflection: max 1%
Valencia	450*130	3.5	3.50	10	Aluminum, 20 mm (bottom) Acrylic, 50 mm (top)	
Zurich	400*106	3.8	3.48	10	Aluminum (bottom) Glass (top) + aluminum stiffening structure (150 mm)	Thickness variation: 1.4% Mold deflection: ⩽2.9% (at 4 bars)

Table 5
Details on injection pressures and flow detection techniques.

Institution	Monitoring injection pressure	Initial injection pressure (bar)	Final injection pressure (bar)	Flow detection	Sampling rate/Sensitivity
CCHP	Measured at injection gate	0.85–1.08	0.88–1.11	Human eye + photos	0.5 s
Clausthal	Measured in the mold (averaged)	0.86	0.86	Photos + software	Photos every 5 s
Delaware	–	1.00	1.00	Video	–
INTEMA	Measured at injection gate	0.84–1.38	0.85–1.58	Video	0.5 s
Lausanne	Measured at injection gate	0.60–1.20	0.60–1.29	Human eye	0.5 s
Milwaukee	Flow rate measured at injection gate	$Q = 4.4$ ml/s	–	Human eye + video	0.5 s
Munich	Measured at injection gate	0.91–1.12	1.07–1.40	Human eye + video	0.5 s
Nottingham	Measured at injection gate	1.02–1.13	1.02–1.13	Pressure transducer	0.5 s
PPE	Measured at injection gate	1.01	1.02	Video	0.5 s
Sicomp	Measured at injection gate	0.97–1.00	0.88–0.97	Human eye + video	0.5 s
Valencia	Measured at injection gate	0.86–1.16	1.01–1.28	Human eye + photos	0.5 s
Zurich	Measured at injection gate	0.76–0.93	0.92–0.97	Human eye + photos	Photos every 2.35 s

erties for all participants (i.e. similar μ, γ and θ), the only parameter left is the flow velocity which depends on injection pressure. For a constant pressure experiment, the flow front velocity decreases with the unsaturated flow advancement. The capillary effects resulting from this velocity evolution are included in the unsaturated permeability measurement without a possible identification. Since the flow lengths of the participants are similar, the same injection pressure was fixed to ensure an identical contribution of these capillary effects. It was agreed that a relative injection pressure of 1 bar would be representative of the processing of the carbon fabric to be tested. As presented in Table 5, most participants measured an injection pressure between 0.60 and 1.58 bars. Only Milwaukee used a constant flow rate injection unit that did not allow controlling pressure.

In this exercise, there was no particular specification regarding the flow front detection. Numerous techniques exist to perform the flow front tracking such as the use of fiber optic sensors [33], pressure transducers [34] or ultrasound measurement [35]. However, the most commonly employed method remains the visual monitoring through a transparent mold [5,36]. In order to reduce the scatter and solve statistical equations described in the next section, it was recommended to measure multiple data points during testing. As displayed in Table 5, most of the participants have opted for the visual tracking of the flow front. Nottingham has chosen a pressure transducer to detect the flow front position in a closed mold and implemented a fully automated measurement and evaluation procedure. In this case, the permeability was computed using the single point method [30] which does not allow any correcting scheme (such as least square fit). Milwaukee has injected the testing fluid at a constant flow rate. Thus, a saturated permeability was estimated by measuring the pressure drop across the preform, not applying the equations presented below.

2.3. Permeability calculations

To calculate the permeability of a fibrous reinforcement, it is important to know and control the fiber volume fraction of the preform. This fiber volume fraction is directly connected to the total mass of fiber m_f (of all the fabric layers), the length l and the width w of the preform, the mold cavity height h and the volumetric density of the fiber ρ_f:

$$V_f = \frac{m_f}{l \cdot w \cdot h \cdot \rho_f} \qquad (4)$$

The free porosity Φ of the fibrous reinforcement can be thus calculated as:

$$\Phi = 1 - V_f \qquad (5)$$

2.3.1. Unidirectional permeability calculation

Two different techniques were used to determine the unidirectional permeability of the fabric in each direction. Both methods require injecting the test fluid at a constant pressure P_{inj}. The first one is based on an interpolation of the flow front position during the injection. According to Darcy's law, a linear trend can be fitted when plotting the Squared Flow Front position against the time. The permeability of a fibrous reinforcement can then be computed as follows:

$$K_{SFF} = \frac{x_{ff}^2 \cdot \Phi \cdot \mu}{2 \cdot P_{inj} \cdot t} = \frac{m \cdot \Phi \cdot \mu}{2 \cdot P_{inj}} \qquad (6)$$

where x_{ff} corresponds to the flow front position at the instant t, which can be replaced by the slope m interpolated from the coupled data $\left(x_{ff}^2, t \right)$. This approach will be referred to as the Squared Flow Front method (SFF method) in this paper.

The second technique used to compute the unidirectional permeability is based on a statistical approximation of the experimental data. As described by Ferland et al. [30], a least square fit can be applied to the values of pressure in order to estimate a permeability self-correlated to Darcy's law. Indeed, defining:

$$a = \sqrt{\frac{2 \cdot K}{\Phi \cdot \mu}} \qquad (7)$$

and applying a least square fit on the approximated integral of the pressure I_i gives:

$$a = \frac{\sum_{i=1}^{n} x_{ff,i} \cdot \sqrt{I_i}}{\sum_{i=1}^{n} I_i} \qquad (8)$$

with:

$$I_i = I_{i-1} + \frac{(P_{inj,i} - P_{inj,i-1})}{2}(t_i - t_{i-1}) \qquad (9)$$

Finally, the Least Square Fit permeability (LSF method) is determined substituting Eq. (8) in (7):

$$K_{LSF} = \left(\frac{\sum_{i=1}^{n} x_{ff,i} \cdot \sqrt{I_i}}{\sum_{i=1}^{n} I_i} \right)^2 \frac{\Phi \cdot \mu}{2} \qquad (10)$$

2.3.2. Principal permeability calculation

Once the scalar value of permeability of the fibrous reinforcement in the three different directions (0°, 45° and 90°) is obtained, it is possible to calculate the in-plane permeability tensor K_1 and K_2 as follows [5]:

$$K_1 = K_{exp}^0 \frac{\alpha_1 - \alpha_2}{\alpha_1 - \frac{\alpha_2}{\cos(2\beta)}} \qquad (11)$$

and

$$K_2 = K_{exp}^{90} \frac{\alpha_1 + \alpha_2}{\alpha_1 + \frac{\alpha_2}{\cos(2\beta)}} \tag{12}$$

where α_1 and α_2 are written as:

$$\alpha_1 = \frac{K_{exp}^0 + K_{exp}^{90}}{2} \tag{13}$$

$$\alpha_2 = \frac{K_{exp}^0 - K_{exp}^{90}}{2} \tag{14}$$

and the orientation β of the ellipse is:

$$\beta = \frac{1}{2} \tan^{-1} \left(\frac{\alpha_1}{\alpha_2} - \frac{\alpha_1^2 - \alpha_2^2}{\alpha_2 \cdot K_{exp}^{45}} \right) \tag{15}$$

2.3.3. Error calculation

The uncertainty in calculation of K_1, K_2 and β can be estimated according to two different methods: using the law of error propagation [34] or using the exact total differential. Both calculations have advantages and drawbacks: the first one is easy to calculate but depends on values not always easy to estimate while the second one depends only on effective experimental values of permeability but is more complex to develop. In the first benchmark, the law of error propagation was applied. However, uncertainties on several principal permeability data were not calculated because some information was missing. In this work, for a better comparison, the exact total differentials were calculated for K_1, K_2 and β. Eq. (16) displays the exact total differential of β.

$$d\beta = \left| \frac{\partial \beta}{\partial K_{exp}^0} \right| \cdot dK_{exp}^0 + \left| \frac{\partial \beta}{\partial K_{exp}^{45}} \right| \cdot dK_{exp}^{45} + \left| \frac{\partial \beta}{\partial K_{exp}^{90}} \right| \cdot dK_{exp}^{90} \tag{16}$$

with, for example:

$$\frac{\partial \beta}{\partial K_{exp}^0} = \frac{K_{exp}^{45} \cdot K_{exp}^{90} \left(K_{exp}^{90} - K_{exp}^{45} \right)}{K_{exp}^{45^2} \cdot \left(K_{exp}^{0^2} + K_{exp}^{90^2} \right) + 2K_{exp}^0 \cdot K_{exp}^{90} \left(K_{exp}^0 \cdot K_{exp}^{90} - K_{exp}^{45} \left(K_{exp}^0 + K_{exp}^{90} \right) \right)} \tag{17}$$

The results obtained were compared with the law of propagation for Nottingham. Uncertainties obtained were comparable in both cases even if the law of propagation was slightly more conservative.

3. Results and discussion

3.1. Reinforcement deformability

The permeability measurements were supplemented by the characterization of the deformability of the fabric carried out by the KU Leuven. This information may be helpful in future to improve the interpretation of the permeability data or to carry out numerical simulations. Shear testing was performed with a picture frame [37,38], compression testing was done on the undeformed and sheared fabrics. The results are shown in Fig. 4. The important deformability features of the studied fabric are:

- very low shear resistance, which up to a shear angle of 45° is completely defined by low friction in the yarn intersections
- locking shear angle above 50°
- pronounced nesting effect, with a decrease of the effective thickness of the ply in a four-plies laminate by 15–20% compared to one-ply thickness

was done on the undeformed and sheared fabrics. The results are shown in Fig. 4. The important deformability features of the studied fabric are:
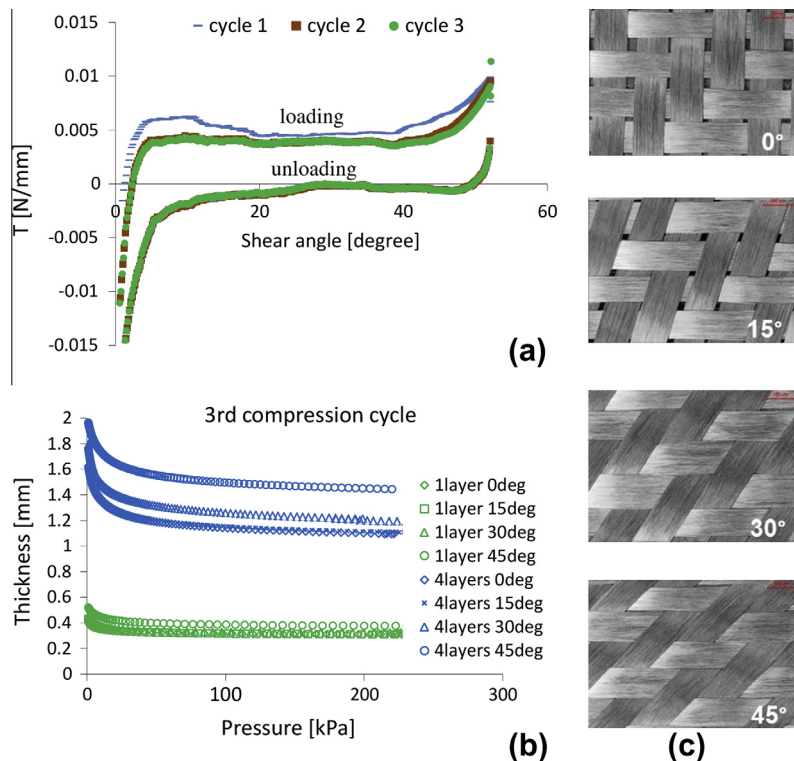

Fig. 4. Fabric deformability: (a) shear diagrams: shear force *T* vs. shear angle; (b) compression diagrams: fabric thickness vs. pressure (c) images of the sheared fabric. (For interpretation of the references to colour in this figure legend, the reader is referred to the web version of this article.)

3.2. Effective permeability results

The effective permeability values measured by all participants are displayed in Figs. 5–7 and the data is presented in Tables A1–A3. All the participants have used the SFF and LSF methods to calculate the permeability in each direction except for Nottingham and Milwaukee. They have implemented other methods as their setup is different from that of other institutions (see Section 2.2 for details). For Nottingham, only one calculation of permeability was available while for Milwaukee, two values were obtained: in the steady-state condition (in SFF column) and in the transient condition (in LSF column). The choice to put these values in these columns is arbitrary but does not affect the comparison since they are almost identical.

Tables A1–A3 also present two different arithmetic means calculated as follows: (a) the average permeability values of participants who respected the recommendations (all institutions except Delaware, Nottingham and Milwaukee) and (b) the average permeability values of all participants. For each case, the coefficient of variation c_v is calculated using the standard deviation σ and the arithmetic mean m_e:

$$c_v = \frac{\sigma}{m_e} \tag{18}$$

Regarding Figs. 5–7, the unique value obtained by Nottingham is displayed in both SFF and LSF graphs. For one participant (Lausanne), the average value and standard deviation were calculated despite only two experiments having been performed in each direction. This statistical evaluation of the data is questionable since permeability measurements have a significant variability. A greater number of tests were carried out from other institutions allowing better statistical evaluation.
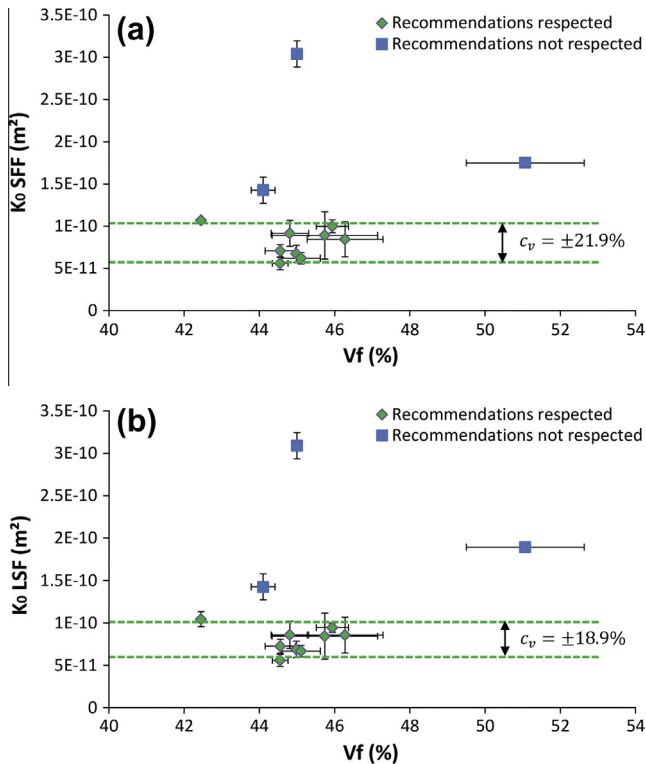

Fig. 5. Effective permeability along the warp direction (0°) calculated using: (a) the SFF method and (b) the LSF method. (For interpretation of the references to colour in this figure legend, the reader is referred to the web version of this article.)

Fig. 6. Effective permeability along 45° calculated using: (a) the SFF method and (b) the LSF method. (For interpretation of the references to colour in this figure legend, the reader is referred to the web version of this article.)
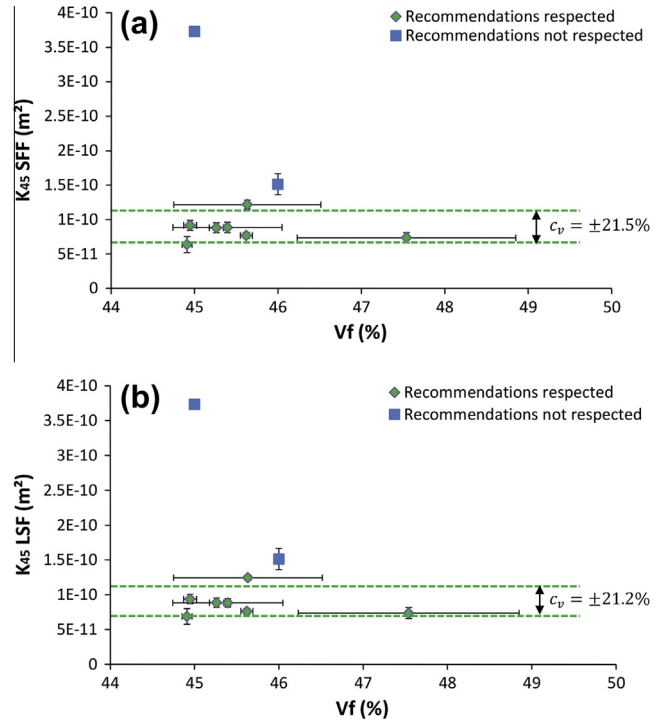

Fig. 7. Effective permeability along the weft direction (90°) calculated using: (a) the SFF method and (b) the LSF method. (For interpretation of the references to colour in this figure legend, the reader is referred to the web version of this article.)
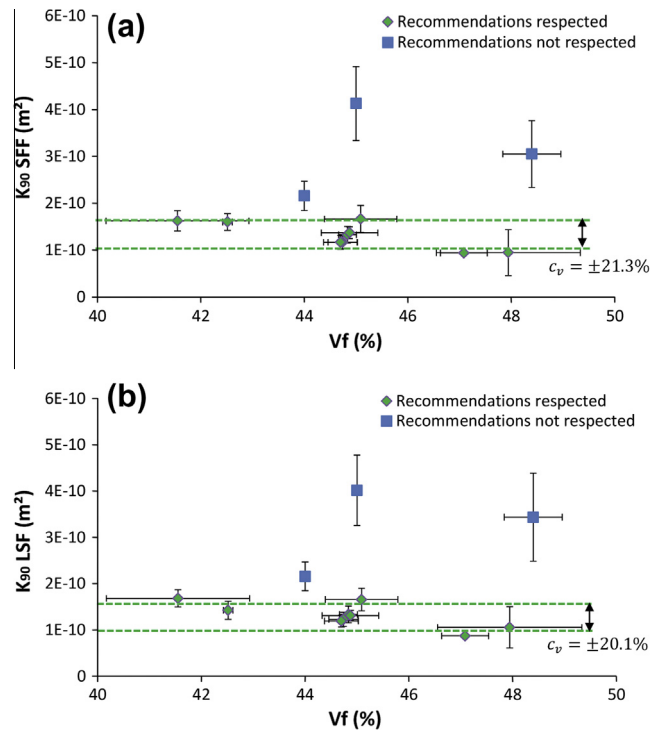
3.2.1. Results in the warp direction (0°)

Fig. 5(a) and (b) show respectively to the results obtained at 0° with the SFF and LSF methods as presented in Table A1. For both

methods, the permeability values of participants respecting the recommendations are very close, with a lower variability for the LSF method. For these nine institutions, the scatter may represent the uncertainty of the fiber volume fraction, fiber nesting and the testing technique. When respecting the guidelines (nine participants), the estimated error on the standard deviation is only ±22% for the SFF method and ±19% for LSF, which is very low considering that these tests were carried out by different institutions. Coefficients of variation calculated for these participants from their own data are generally around 15%. It means that the variability observed between each setup is almost comparable to the variability of the setups themselves in this direction. The value obtained by Nottingham and Delaware are slightly upper to that of other participants while for Milwaukee, the value is approximately three times higher.

3.2.2. Results in the direction 45°

Displayed in Fig. 6(a) and (b) are the results obtained at 45° with the SFF and LSF methods respectively. These results are also available in Table A2. Even if less data are available in this direction, some interesting remarks can be inferred. Again, SFF and LSF methods give comparable results with less scatter for the LSF method. The standard deviations of the permeability in this direction are lower than along 0°. Some participants had difficulties in controlling the fiber volume fraction of the samples, probably because the cutting of the fabric posed problems. Indeed, as presented in the previous section on reinforcement characterization, the fabric can be sheared very easily until an angle of almost 40°. Cutting the sample at 45° is then more laborious than at 0° and 90° since the fabric shears during cutting, thus varying the areal density of the sample and consequently the fiber volume fraction. The scatter of experimental data in this direction is in the same range as for the effective permeability along 0°. The coefficient of variation in this direction is comparable to the one obtained along 0° (around 22%). The same scatter as observed previously is obtained between Nottingham and Milwaukee values, and that of other participant.

3.2.3. Results in the weft direction (90°)

Fig. 7(a) and (b) show the permeability results at 90° obtained with the SFF and LSF methods respectively. These values are also available in Table A3. Both methods give comparable results with again lower scatter for the LSF method. In this direction, a higher variation of fiber volume fraction is observed. In fact, five values are near 45% while other results are around 42% and 48%. However, the variability between institutions is about the same as at 0° and 45° (coefficient of variation on the mean around 21%). The permeability values obtained by Nottingham, Delaware and Milwaukee are slightly higher than those from the other participants. However these institutions did not follow the recommendations as they used their existing setup.

3.2.4. General remarks

The SFF and LSF methods give similar results for each direction. The LSF technique systematically shows a lower dispersion than the SFF method. The variation of the mean permeability values of each participant when the recommendations are respected is around 15% for each direction. The coefficient of variation considering all institutions is also very low (around 21%). The scatter between each institution is comparable to the scatter of each institution, which suggests robustness of the proposed technique to characterize the permeability of fibrous reinforcements.

As already observed in the first benchmark, results obtained from setups with different specifications contrast those from setups that respect the guidelines of the present benchmark. Milwaukee obtained 3 times higher permeability while the values

of Delaware and Nottingham were around 1.5–2.5 times higher. This difference may arise from the way the permeability was calculated by Milwaukee and Nottingham, but not by Delaware. The constant flow rate procedure used by Milwaukee is hardly comparable to others. The method of flow front detection is different for Nottingham and the permeability was calculated by the single point method. The only common difference with other participants is the injected fluid. In fact, all the other institutions have used silicone oil while the measurements were carried out by Delaware, Milwaukee and Nottingham with corn syrup, motor oil and synthetic oil respectively. Despite this observation, it cannot be concluded here that the testing fluid is responsible of the observed scatter. New measurements on the same setup with silicone oil would be needed to validate this hypothesis.

3.3. Principal permeability results

To calculate the in-plane permeability tensor of the fabric, it is necessary to have unidirectional permeability measurements in each of the three directions (i.e. 0°, 45° and 90°). Thus, the participants who did not perform tests in all the three directions could not obtain the permeability tensor. Hence, only nine institutions were able to provide sufficient data to perform tensor calculations.

In Figs. 8–11, values of K_1, K_2, K_1/K_2 and β for each participant are displayed respectively. The error bars displayed in these figures are calculated by Eq. (16). Tables A4 and A5 summarize these data for the SFF and LSF approaches respectively. At the bottom of these tables the average values of participants who respected the guidelines (all institutions except Delaware, Nottingham and Milwaukee) and the average values of all participants are presented.

3.3.1. Principal permeability K_1

Fig. 8(a) and (b) show the principal permeability K_1 calculated from effective permeability obtained via the SFF and LSF methods
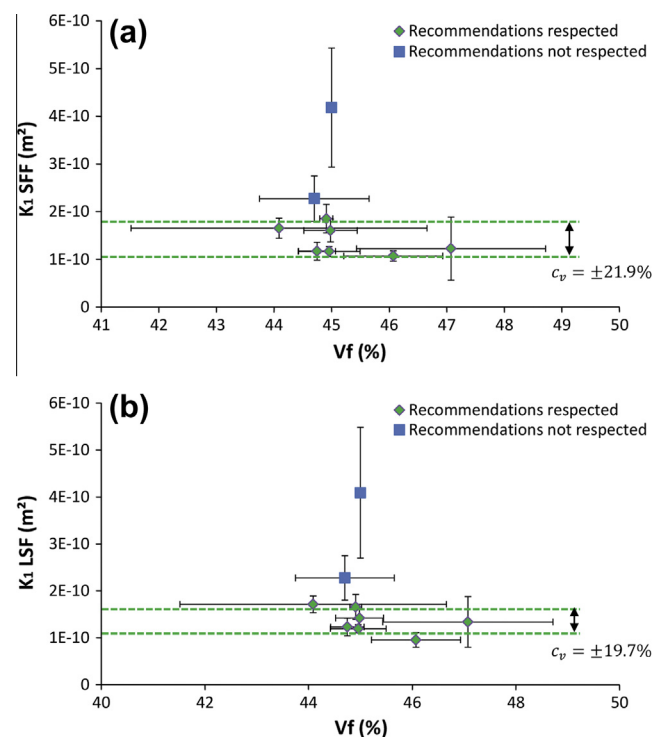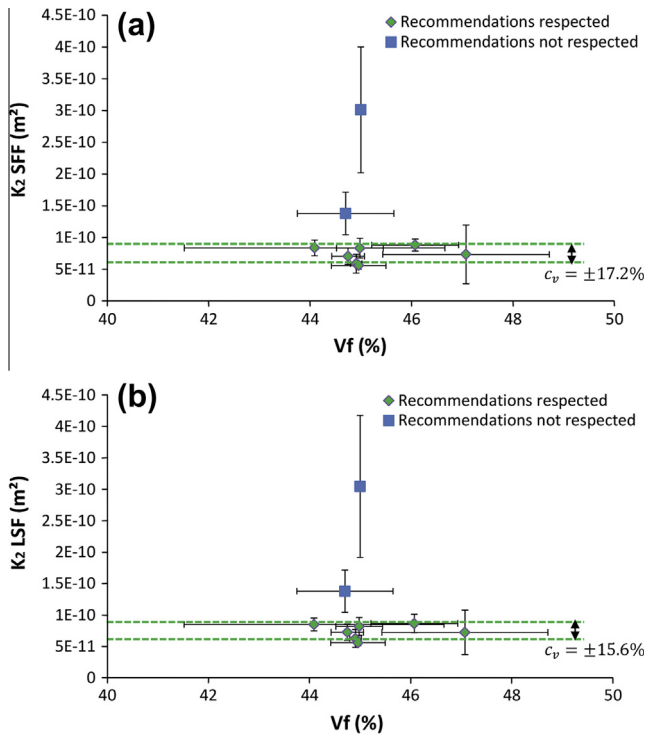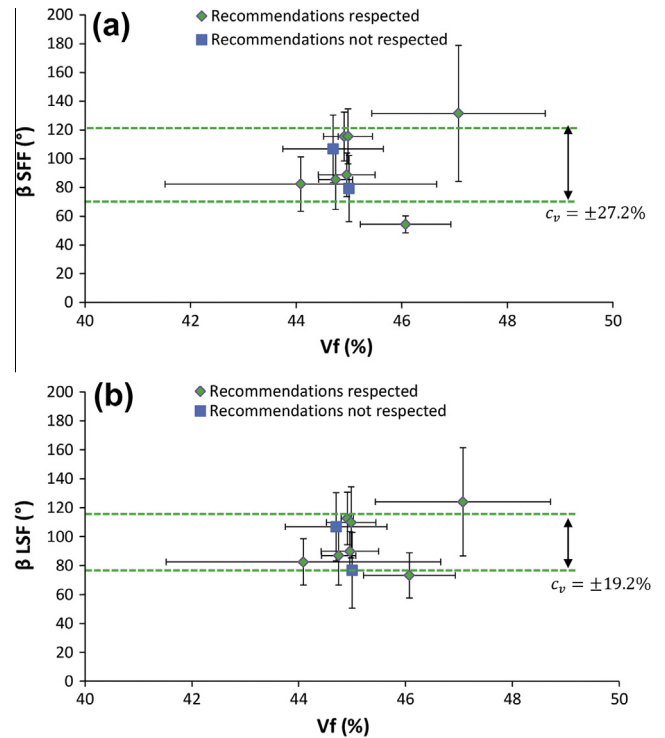

Fig. 8. Principal permeability K_1 obtained using: (a) the SFF method and (b) the LSF method. (For interpretation of the references to colour in this figure legend, the reader is referred to the web version of this article.)
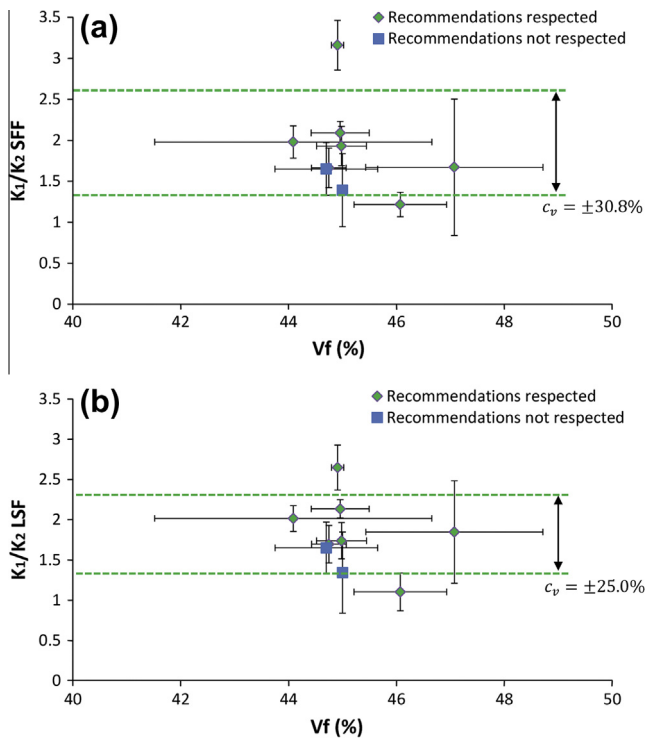
Fig. 9. Principal permeability K_2 obtained using: (a) the SFF method and (b) the LSF method. (For interpretation of the references to colour in this figure legend, the reader is referred to the web version of this article.)

Fig. 10. Anisotropy ratio K_1/K_2 obtained using: (a) the SFF method and (b) the LSF method. (For interpretation of the references to colour in this figure legend, the reader is referred to the web version of this article.)

respectively. The exact values are available in Tables A4 and A5. An averaged permeability K_1 of $1.4 * 10^{-10}$ m^2 was obtained for all participants that respected the guidelines of this exercise. This re-

Fig. 11. Angle β obtained using: (a) the SFF method and (b) the LSF method. (For interpretation of the references to colour in this figure legend, the reader is referred to the web version of this article.)

sult is similar for both the approaches used to compute effective permeability values SFF and LSF. However, the LSF approach gives lower scatter than the SFF approach (22% for SFF versus 20% for LSF).

3.3.2. Principal permeability K_2

The principal permeability K_2 calculated from effective permeability obtained via the SFF and LSF methods for each participant is displayed in Fig. 9(a) and (b) respectively. The exact values are also available in Tables A4 and A5. An averaged principal permeability K_2 of $7.3 * 10^{-11}$ m^2 was obtained from both SFF and LSF approaches (guidelines respected). Permeability K_2 is half the value of K_1. This will be analyzed in the K_1/K_2 anisotropy ratio section. These results show that the LSF method still yields less scatter of experimental data. The coefficient of variation of data obtained respecting the recommendations is low (around 16%). It confirms that the scatter of the values for these institutions is negligible in relation to the scatter of values of the experiments conducted at each department.

3.3.3. Anisotropy ratio K_1/K_2

Ratios of anisotropy calculated from the previous values of principal permeability are shown in Fig. 10(a) for the SFF approach and Fig. 10(b) for the LSF method. Values are available in Tables A4 and A5 respectively. The scatter between institutions for the LSF calculation is much lower than when using SFF (31% for SFF and 25% for LSF). The LSF approach has shown to produce less scatter over the effective permeability values than the SFF approach and hence it also results in a better determination of the permeability tensor and the elliptic shape of the in-plane flow. Note that anisotropy ratios obtained by institutions which not respect the recommendations lie in the same range of values than when the recommendations were respected.

3.3.4. Ellipse orientation β

The orientation angle β between the warp direction and the major axis of permeability K_1 for each participant is shown in Fig. 11(a) and (b) for the SFF and LSF approaches respectively. Experimental data are also available in Tables A4 and A5. The averaged elliptic flow determined by all the institutions is around 96° even if two of them did not respect of the recommendations. The variability of the flow orientation from most participants is in the order of ±20°. However, this is not the case for Sicomp, for which a variability of ±37° was observed. This is probably related to the lack of control of V_f and shearing deformation of the fabric during cutting as explained in Section 3.2. Despite this higher variability, the averaged flow directions are still close to other participant results. As for previous results, the LSF approach results in smaller variability than the SFF technique, although both give the same orientation.

4. Comparison with the first permeability benchmark

In the first permeability benchmark exercise [24], a total of 16 different characterization techniques were compared, such as radial or linear injection, saturated or unsaturated flow, constant pressure or flow rate, with different test fluids and at different fiber volume fraction. Each participant was asked to measure permeability using his current set-up and practice. Figs. 12 and 13 display the results of K_1 and K_2 obtained for the first benchmark. The compilation of results from twelve institutions resulted in a high variability of data: permeability measured at similar V_f (close to 45% and 50% for example) varied by more than one order of magnitude. However, the numerous differences between experimental procedures could not be associated to the observed permeability scatter. Consequently it appears difficult to point out the influence of a specific parameter on the permeability. In the conclusions of that benchmark, authors suspected that the human factor could be also responsible for this significant scatter.

The present exercise was based on a common characterization technique followed by nine different institutions. A careful control of injection parameters has permitted to reach a smaller scatter compared to the first benchmark. The variability observed in the second benchmark is also displayed in Figs. 12 and 13 for sake of comparison (guidelines respected). It can be first stated that the average permeability obtained in the second exercise is generally smaller than in the first benchmark near a fiber volume fraction of 45%. This could be explained by the difference in the experimental procedures followed; however, it is difficult to reach a conclusion because of the diversity of methods used in the first
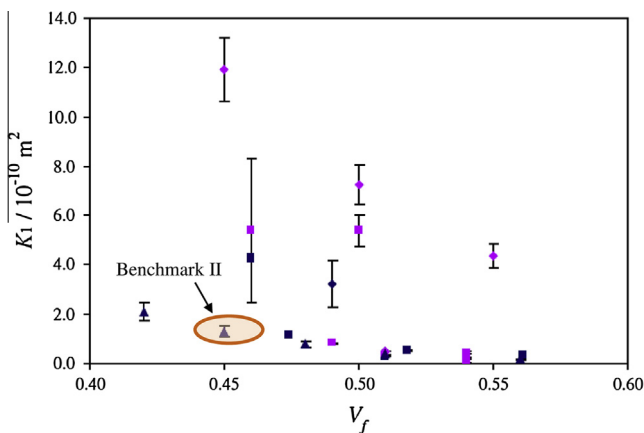

Fig. 12. Principal permeability K_1 obtained in the first permeability benchmark [24] and comparison with current benchmark. (For interpretation of the references to colour in this figure legend, the reader is referred to the web version of this article.)

Fig. 13. Principal permeability K_2 obtained in the first permeability benchmark [24] and comparison with current benchmark. (For interpretation of the references to colour in this figure legend, the reader is referred to the web version of this article.)
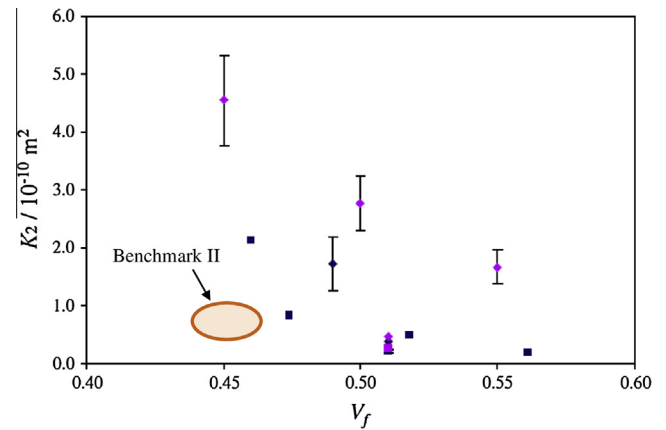
exercise. The scatter of experimental data is also one order of magnitude smaller than in the first exercise. This applies to the principal permeability K_1 and K_2. The ellipse orientation β was defined in the second benchmark as the angle between the warp direction of the fabric and the major permeability axis. In the first benchmark, it was described as the angle between the weft direction of the fabric and the major axis. Thus, to compare both results, 90° has to be added to the angle of the first benchmark. Finally, an ellipse orientation of approximately 90° was found in both benchmarks.

5. Summary and concluding remarks

The aim of this second permeability benchmark was to measure and compare the permeability of a carbon fabric using a specified procedure. A total of 13 institutions have participated on this exercise worldwide. One institution has investigated the geometrical parameters and deformations of the chosen carbon fabric while the others have measured the in-plane permeability.

The unidirectional unsaturated permeability of the fabric was characterized in three directions (0°, 45° and 90°). Parameters such as the test fluid, the injection pressure, the fiber volume fraction, etc. were set in order to eliminate their effect on the variability of the measured values. Defining the test fluid is mainly based on the fact that capillary flow plays a key role on the saturation of fiber tows and hence on the unsaturated permeability values. This was done by specifying the test fluid to be silicone oil with a viscosity of 0.1 Pa s, and the injection pressure of 1 bar. In addition, sample dimensions, aspect ratio and fiber volume fraction were also specified in the proposed exercise. A series of templates were created so that each participant could carry out the permeability calculations according to the same set of formulae. Finally, the experimental data from the participating institutions were compiled and presented in this paper.

As a result of this exercise, an averaged permeability of $1.4 * 10^{-10}$ m^2 was obtained in the principal direction of the carbon fabric. In the minor axis direction, an averaged permeability of $0.7 * 10^{-10}$ m^2 was obtained. In both cases, a standard deviation of ±20% was calculated from the data of seven participants. Two techniques were used to determine permeability from the experimental. The first approach called Squared Flow Front (SFF) consists of a linear regression over the square of the flow front positions in time. The second approach named Least Square Fit (LSF) uses a statistical solution to compute the permeability over a range of data. The results of this exercise demonstrate that a smaller scatter is systematically obtained with the LSF method. However, in all

cases, the SFF approach gave nearly the same average values as the LSF approach, but with a higher scatter.

From the twelve participants that reported permeability data, three of them were unable to follow the guidelines and recommendations because of the design of their experimental setups. These three institutions obtained permeability data that were significantly off the average of the other participants. This indicates that the recommendations in the guideline document do in fact assist in obtaining a reproducible permeability value allowing future test standardization.

A comparison was also performed with the first permeability benchmark carried out in 2009. This first exercise did not specify any recommendation and allowed the participants to follow their own specifications and methods. As a result, a large scatter of more than one order of magnitude was observed. Comparing the results of the two benchmarks, it was demonstrated that this second exercise leads to a much smaller scatter in the determination of the permeability tensor for a given fiber volume fraction. This observation supports the assumption of this exercise that controlling the test conditions (injection pressure, test fluid, fiber volume fraction,

Table A1
Effective permeability values of each participant in direction 0°.

Institution	N_{exp}	V_f (%)	$K_{SFF\ 0°}$ (10^{-10} m^2) ($\pm c_v$)	$K_{LSF\ 0°}$ (10^{-10} m^2) ($\pm c_v$)
CCHP	10	44.6 ± 0.4	0.705 ± 0.074 (±10.5%)	0.725 ± 0.082 (±11.3%)
Clausthal	7	45.0 ± 0.1	0.671 ± 0.101 (±15.1%)	0.688 ± 0.098 (±14.3%)
Delaware[*]	3	51.1 ± 1.6	1.748 ± 0.041 (±2.4%)	1.892 ± 0.031 (±1.7%)
INTEMA	6	46.3 ± 1.0	0.842 ± 0.207 (±24.6%)	0.856 ± 0.210 (±24.5%)
Lausanne	2	42.5	1.068 ± 0.013 (±1.3%)	1.043 ± 0.088 (±8.4%)
Milwaukee[*]	4	45	3.040 ± 0.155 (±5.1%)	3.088 ± 0.153 (±4.9%)
Munich	7	44.8 ± 0.5	0.913 ± 0.154 (±16.9%)	0.858 ± 0.160 (±18.7%)
Nottingham[*]	10	44.1 ± 0.3	1.425 ± 0.154 (±10.8%)	
PPE	10	45.9 ± 0.4	0.997 ± 0.077 (±7.8%)	0.944 ± 0.054 (±5.7%)
Sicomp	10	45.7 ± 1.4	0.889 ± 0.564 (±31.4%)	0.844 ± 0.272 (±32.2%)
Valencia	10	45.1 ± 0.5	0.614 ± 0.047 (±7.6%)	0.683 ± 0.048 (±7.0%)
Zurich	9	44.6 ± 0.2	0.558 ± 0.076 (±13.7%)	0.558 ± 0.070 (±12.6%)
Mean (reco. resp.)		44.9 ± 1.1	0.807 ± 0.177 (±21.9%)	0.798 ± 0.151 (±18.9%)
Mean (all results)		45.4 ± 2.0	1.123 ± 0.695 (±61.8%)	1.132 ± 0.718 (±63.4%)

[*] Guidelines not respected.

Table A2
Effective permeability values of each participant in direction 45°.

Institution	N_{exp}	V_f (%)	$K_{SFF\ 45°}$ (10^{-10} m^2) ($\pm c_v$)	$K_{LSF\ 45°}$ (10^{-10} m^2) ($\pm c_v$)
CCHP	10	45.0 ± 0.1	0.915 ± 0.074 (±8.0%)	0.937 ± 0.068 (±7.3%)
Clausthal	8	44.9 ± 0.1	0.635 ± 0.116 (±18.2%)	0.687 ± 0.113 (±16.5%)
Delaware[*]	0			
INTEMA	3	45.6 ± 0.9	1.215 ± 0.066 (±5.4%)	1.243 ± 0.039 (±3.2%)
Lausanne	0			
Milwaukee[*]	4	45.0	3.725 ± 0.037 (±1.0%)	3.734 ± 0.048 (±1.3%)
Munich	6	45.3 ± 0.1	0.879 ± 0.071 (±8.1%)	0.885 ± 0.067 (±7.6%)
Nottingham[*]	10	46.0	1.511 ± 0.153 (±10.1%)	
PPE	10	45.4 ± 0.7	0.885 ± 0.077 (±8.7%)	0.882 ± 0.060 (±6.8%)
Sicomp	10	47.5 ± 1.3	0.734 ± 0.164 (±10.0%)	0.735 ± 0.080 (±10.8%)
Valencia	0			
Zurich	10	45.6 ± 0.1	0.767 ± 0.043 (±5.6%)	0.762 ± 0.040 (±5.2%)
Mean (reco. resp.)		45.6 ± 0.9	0.861 ± 0.185 (±21.5%)	0.876 ± 0.186 (±21.2%)
Mean (all results)		45.6 ± 0.8	1.252 ± 0.966 (±77.1%)	1.264 ± 0.963 (±76.2%)

[*] Guidelines not respected.

Table A3
Effective permeability values of each participant in direction 90°.

Institution	N_{exp}	V_f (%)	$K_{SFF\ 90°}$ (10^{-10} m^2) ($\pm c_v$)	$K_{LSF\ 90°}$ (10^{-10} m^2) ($\pm c_v$)
CCHP	10	44.7 ± 0.3	1.165 ± 0.135 (±11.6%)	1.225 ± 0.151 (±12.3%)
Clausthal	6	44.8 ± 0.2	1.326 ± 0.177 (±13.3%)	1.332 ± 0.182 (±13.6%)
Delaware[*]	5	48.4 ± 0.6	3.050 ± 0.716 (±23.5%)	3.435 ± 0.952 (±27.7%)
INTEMA	7	41.6 ± 1.4	1.623 ± 0.216 (±13.3%)	1.681 ± 0.186 (±11.1%)
Lausanne	2	42.5 ± 0.1	1.599 ± 0.177 (±11.1%)	1.424 ± 0.196 (±13.8%)
Milwaukee[*]	4	45.0	4.127 ± 0.791 (±19.2%)	4.014 ± 0.760 (±18.9%)
Munich	7	44.9 ± 0.6	1.369 ± 0.127 (±9.3%)	1.309 ± 0.112 (±8.6%)
Nottingham[*]	10	44.0	2.156 ± 0.310 (±14.4%)	
PPE	6	47.1 ± 0.3	0.935 ± 0.010 (±1.1%)	0.866 ± 0.018 (±2.1%)
Sicomp	10	47.9 ± 1.4	0.946 ± 1.220 (±51.7%)	1.055 ± 0.446 (±42.3%)
Valencia	10	45.1 ± 0.7	1.624 ± 0.274 (±16.9%)	1.644 ± 0.229 (±14.0%)
Zurich	8	44.7 ± 0.3	1.165 ± 0.148 (±12.7%)	1.191 ± 0.128 (±10.8%)
Mean (reco. resp.)		44.8 ± 2.0	1.311 ± 0.280 (±21.3%)	1.305 ± 0.262 (±20.1%)
Mean (all results)		45.1 ± 2.0	1.761 ± 0.947 (±53.8%)	1.779 ± 0.975 (±54.8%)

[*] Guidelines not respected.

Table A4
Principal permeability values, anisotropy ratio and ellipse orientation calculated with SFF method.

Institution	V_f (%)	$K_{1\ SFF}$ $(10^{-10}\ m^2)$ $(\pm c_v)$	$K_{2\ SFF}$ $(10^{-10}\ m^2)$ $(\pm c_v)$	$K_{1\ SFF}/K_{2\ SFF}$ $(\pm c_v)$	β_{SFF} (°) $(\pm c_v)$
CCHP	44.8 ± 0.3	1.170 ± 0.186 (±15.9%)	0.704 ± 0.129 (±18.3%)	1.663 ± 0.242 (±14.6%)	85.5 ± 20.8 (±24.3%)
Clausthal	44.9 ± 0.1	1.853 ± 0.302 (±16.3%)	0.587 ± 0.149 (±25.4%)	3.160 ± 0.301 (±9.5%)	115.4 ± 17.0 (±14.8%)
*Delaware**					
INTEMA	44.1 ± 2.6	1.652 ± 0.211 (±12.8%)	0.835 ± 0.125 (±15.0%)	1.979 ± 0.197 (±10.0%)	82.3 ± 18.9 (±22.9%)
Lausanne					
Milwaukee*	45.0	4.184 ± 1.251 (±29.9%)	3.010 ± 0.990 (±32.9%)	1.390 ± 0.445 (±32.0%)	79.2 ± 23.0 (±29.0%)
Munich	45.0 ± 0.5	1.605 ± 0.241 (±15.0%)	0.832 ± 0.156 (±18.8%)	1.929 ± 0.240 (±12.4%)	115.5 ± 19.1 (±16.5%)
Nottingham*	44.7 ± 1.0	2.273 ± 0.475 (±20.9%)	1.378 ± 0.336 (±24.4%)	1.649 ± 0.321 (±19.5%)	106.8 ± 23.6 (±22.1%)
PPE	46.1 ± 0.9	1.070 ± 0.110 (±10.3%)	0.880 ± 0.096 (±10.9%)	1.215 ± 0.150 (±12.3%)	54.3 ± 5.9 (±10.9%)
Sicomp	47.1 ± 1.5	1.224 ± 0.662 (±54.1%)	0.733 ± 0.463 (±63.1%)	1.670 ± 0.831 (±49.8%)	131.5 ± 47.3 (±35.9%)
Valencia					
Zurich	45.0 ± 0.1	1.166 ± 0.104 (±8.9%)	0.558 ± 0.060 (±10.7%)	2.090 ± 0.139 (±6.7%)	88.7 ± 15.1 (±17.0%)
Mean (reco. resp.)	45.3 ± 1.0	1.391 ± 0.305 (±21.9%)	0.733 ± 0.126 (±17.2%)	1.958 ± 0.603 (±30.8%)	96.2 ± 26.2 (±27.2%)
Mean (all results)	45.2 ± 0.9	1.800 ± 0.977 (±54.3%)	1.057 ± 0.771 (±72.9%)	1.861 ± 0.561 (±30.1%)	95.5 ± 23.7 (±24.9%)

* Guidelines not respected.

Table A5
Principal permeability values, anisotropy ratio and ellipse orientation calculated with LSF method.

Institution	V_f (%)	$K_{1\ LSF}$ $(10^{-10}\ m^2)$ $(\pm c_v)$	$K_{2\ LSF}$ $(10^{-10}\ m^2)$ $(\pm c_v)$	$K_{1\ LSF}/K_{2\ LSF}$ $(\pm c_v)$	β_{LSF} (°) $(\pm c_v)$
CCHP	44.8 ± 0.3	1.228 ± 0.187 (±15.2%)	0.724 ± 0.128 (±17.7%)	1.696 ± 0.233 (±13.8%)	86.9 ± 20.3 (±23.4%)
Clausthal	44.9 ± 0.1	1.655 ± 0.264 (±16.0%)	0.625 ± 0.143 (±22.8%)	2.649 ± 0.279 (±10.5%)	112.6 ± 18.2 (±16.2%)
*Delaware**					
INTEMA	44.1 ± 2.6	1.710 ± 0.178 (±10.4%)	0.849 ± 0.103 (±12.1%)	2.015 ± 0.160 (±7.9%)	82.5 ± 16.0 (±19.4%)
Lausanne					
Milwaukee*	45.0	4.087 ± 1.393 (±34.1%)	3.046 ± 1.131 (±37.1%)	1.342 ± 0.504 (±37.6%)	76.7 ± 26.3 (±34.2%)
Munich	45.0 ± 0.5	1.419 ± 0.205 (±14.4%)	0.817 ± 0.142 (±17.4%)	1.738 ± 0.226 (±13.0%)	109.8 ± 24.6 (±22.4%)
Nottingham*	44.7 ± 1.0	2.273 ± 0.475 (±20.9%)	1.378 ± 0.336 (±24.4%)	1.649 ± 0.321 (±19.5%)	106.8 ± 23.6 (±22.1%)
PPE	46.1 ± 0.9	0.952 ± 0.157 (±16.5%)	0.864 ± 0.146 (±16.9%)	1.102 ± 0.236 (±21.4%)	73.2 ± 16.7 (±21.4%)
Sicomp	47.1 ± 1.5	1.334 ± 0.540 (±40.5%)	0.723 ± 0.355 (±49.1%)	1.846 ± 0.636 (±34.5%)	124.0 ± 37.4 (±30.2%)
Valencia					
Zurich	45.0 ± 0.1	1.191 ± 0.087 (±7.3%)	0.558 ± 0.049 (±8.8%)	2.134 ± 0.114 (±5.4%)	89.8 ± 13.6 (±15.1%)
Mean (reco. resp.)	45.3 ± 1.0	1.356 ± 0.266 (±19.7%)	0.737 ± 0.115 (±15.7%)	1.883 ± 0.471 (±25.0%)	97.0 ± 18.6 (±19.2%)
Mean (all results)	45.2 ± 0.9	1.761 ± 0.952 (±54.1%)	1.065 ± 0.779 (±73.2%)	1.797 ± 0.449 (±25.0%)	98.8 ± 17.9 (±18.7%)

* Guidelines not respected.

etc.) allows a reproducible characterization of the unsaturated permeability of fabrics used in composite manufacturing. The first benchmark concluded that the human factor was responsible of a significant part of the scatter. However this second benchmark strongly suggests that differences between experimental procedures may be responsible of this scatter. Indeed, as the dispersion of the data between all participants is almost equivalent to the dispersion observed for of them. Thus, the human factor appears negligible compared to influence of the test conditions.

The guidelines developed for this exercise summarize the key factors to be taken into account for proper permeability characterization. However, the method proposed here allows only a comparison between unsaturated unidirectional permeability measurements. Since these values depend on the capillary number, different results could be obtained for different test conditions or fluids.

Appendix A

(See Tables A1–A5).

References

[1] ESI Group International Ltd.
[2] Simacek P, Advani SG. Modeling and simulation of resin flow in resin infusion processes such as VARTM, VAP and compression RTM. In: 38th SAMPE Fall Technical Conference: Global Advances in Materials and Process Engineering, November 6, 2006–November 9, 2006. Dallas, TX, United states: Soc. for the Advancement of Material and Process Engineering; 2006.
[3] Polyworx inc.
[4] Darcy H. The public fountains of the city of Dijon. Paris: Dalmont; 1856.
[5] Demaria C, Ruiz E, Trochu F. In-plane anisotropic permeability characterization of deformed woven fabrics by unidirectional injection. Part I: experimental results. Polym Compos 2007;28(6):797–811.
[6] Carman PC. Fluid flow through granular beds. Trans Inst Chem Eng 1937;15(suppl.):150–6.
[7] Gebart BR. Permeability of unidirectional reinforcements for RTM. J Compos Mater 1992;26(8):1100–33.
[8] Lundstrom TS. Permeability of non-crimp stitched fabrics. Composites Part A 2000;31:1345–53.
[9] Papathanasiou TD. Flow across structured fiber bundles: a dimensionless correlation. IJMF 2001;27:1451–61 (Copyright 2001, IEE).
[10] Belov EB, Lomov SV, Verpoest I, Peters T, Roose D, Parnas RS, et al. Modelling of permeability of textile reinforcements: Lattice Boltzmann method. Compos Sci Technol 2004;64(7–8):1069–80.
[11] Verleye B, Lomov SV, Long A, Verpoest I, Roose D. Permeability prediction for the meso-macro coupling in the simulation of the impregnation stage of resin transfer moulding. Composites Part A 2010;41(1):29–35.
[12] Verleye B, Croce R, Griebel M, Klitz M, Lomov SV, Morren G, et al. Permeability of textile reinforcements: simulation, influence of shear and validation. Compos Sci Technol 2008;68(13):2804–10.
[13] Chen Z-R, Ye L, Lu M. Permeability predictions for woven fabric preforms. J Compos Mater 2010;44(13):1569–86.
[14] Masoodi R, Pillai KM, Grahl N, Tan H. Numerical simulation of LCM mold-filling during the manufacture of natural fiber composites. J Reinf Plast Compos 2012;31(6):363–78.

[15] Liu HL, Hwang WR. Permeability prediction of fibrous porous media with complex 3D architectures. Composites Part A 2012;43(11): 2030–8.

[16] Walther J, Simacek P, Advani SG. The effect of fabric and fiber tow shear on dual scale flow and fiber bundle saturation during liquid molding of textile composites. Int J Mater Forming 2012;5(1):83–97.

[17] Sharma S, Siginer DA. Permeability measurement methods in porous media of fiber reinforced composites. Appl Mech Rev 2010;63 (Copyright 2010, The Institution of Engineering and Technology):020802 (19 pp.)..

[18] Kuentzer N, Simacek P, Advani SG, Walsh S. Permeability characterization of dual scale fibrous porous media. Composites Part A 2006;37:2057–68 (Compendex).

[19] Okonkwo K, Simacek P, Advani SG, Parnas RS. Characterization of 3D fiber preform permeability tensor in radial flow using an inverse algorithm based on sensors and simulation. 2011(Compendex).

[20] Adams KL, Miller B, Rebenfeld L. Forced in-plane flow of an epoxy resin in fibrous networks. Polym Eng Sci 1986;26:1434–41 (Compendex).

[21] Bickerton S, Advani SG, Mohan RV, Shires DR. Experimental analysis and numerical modeling of flow channel effects in resin transfer molding. Polym Compos 2000;21(1):134–53.

[22] Parnas RS, Flynn KM, Dal-Favero ME. A permeability database for composites manufacturing. Polym Compos 1997;18(5):623–33.

[23] Lundstrom TS, Stenberg R, Bergstrom R, Partanen H, Birkeland PA. In-plane permeability measurements: a nordic round-robin study. Composites Part A 2000;31A(1):29–43.

[24] Arbter R, Beraud JM, Binetruy C, Bizet L, Breard J, Comas-Cardona S, et al. Experimental determination of the permeability of textiles: a benchmark exercise. Composites Part A 2011;42(9):1157–68.

[25] Alms JB, Correia N, Advani SG, Ruiz E. Experimental procedures to run longitudinal injections to measure unsaturated permeability of LCM reinforcements. FCPM Collaboration 2010.

[26] Dominguez JC, Oliet M, Alonso MV, Rojo E, Rodriguez F. Structural, thermal and rheological behavior of a bio-based phenolic resin in relation to a commercial resol resin. Ind Crops Products 2013;42(1):308–14.

[27] Jiahua Z, Suying W, Yadav A, Zhanhu G. Rheological behaviors and electrical conductivity of epoxy resin nanocomposites suspended with in-situ stabilized carbon nanofibers. Polym Compos 2010;51(12):2643–51.

[28] Alms JB, Correia N, Advani SG, Ruiz E, Gonçalves CT. Experimental procedures to run longitudinal injections to measure unsaturated permeability of LCM reinforcements. 2010.

[29] Lundstrom TS, Gebart BR, Sandlund E. In-plane permeability measurements on fiber reinforcements by the multi-cavity parallel flow technique. Polym Compos 1999;20(1):146–54.

[30] Ferland P, Guittard D, Trochu F. Concurrent methods for permeability measurement in resin transfer molding. Polym Compos 1996;17(1):149–58.

[31] Patel N, Rohatgi V, Lee LJ. Micro scale flow behavior and void formation mechanism during impregnation through a unidirectional stitched fiberglass mat. Polym Eng Sci 1995;35(10):837–51.

[32] LeBel F, Fanaei AE, Ruiz E, Trochu F. Experimental characterization by fluorescence of capillary flows in dual-scale engineering fabrics. Text Res J 2013;83(15):1634–59.

[33] Sung Hoon A, Woo Il L, Springer GS. Measurement of the three-dimensional permeability of fiber preforms using embedded fiber optic sensors. J Compos Mater 1995;29(6):714–33.

[34] Endruweit A, McGregor P, Long AC, Johnson MS. Influence of the fabric architecture on the variations in experimentally determined in-plane permeability values. Compos Sci Technol 2006;66:1778–92 (Compendex).

[35] Luthy T. Three-dimensional permeability measurements based on direct current and ultrasound monitoring techniques. Neuchatel: ETH; 2003.

[36] Luo Y, Verpoest I, Hoes K, Vanheule M, Sol H, Cardon A. Permeability measurement of textile reinforcements with several test fluids. Composites – Part A: Appl Sci Manuf 2001;32(10):1497–504.

[37] Cao J, Akkerman R, Boisse P, Chen J, Cheng HS, de Graaf EF, et al. Characterization of mechanical behavior of woven fabrics: experimental methods and benchmark results. Composites Part A 2008;39(6):1037–53.

[38] Lomov SV, Willems A, Verpoest I, Zhu Y, Barburski M, Stoilova T. Picture frame test of woven composite reinforcements with a full-field strain registration. Text Res J 2006;76(3):243–52.